Transpn. Res.-A, Vol. 24A, No. 5, pp. 345–359, 1990
Printed in Great Britain.

0191-2607/90 $3.00+.00

MODELLING AND REAL-TIME CONTROL OF TRAFFIC FLOW ON THE SOUTHERN PART OF BOULEVARD PERIPHERIQUE IN PARIS: PART I: MODELLING

MARKOS PAPAGEORGIOU
Lehrstuhl für Steuerungs- und Regelungstechnik, Technische Universität München, P.O. Box 202420, D-8000 Munchen 2, Federal Republic of Germany

JEAN-MARC BLOSSEVILLE and HABIB HADJ-SALEM
Institut National de Recherche sur les Transports et leur Sécurité (INRETS), Département Analyse et Régulation du Trafic (DART), 2 Av du Général Malleret-Joinville, 94114-Arcueil Cedex France

(*Received* 16 *February* 1989; *in revised form* 15 *December* 1989)

Abstract—A macroscopic mathematical model of freeway traffic flow is applied to a 6 km stretch of the Boulevard Périphérique in Paris including several on-ramps and off-ramps. The model is validated on the basis of real traffic flow measurements selected under a broad spectrum of traffic conditions. The mathematical model is capable of describing complicated traffic phenomena with considerable accuracy. A simulation program which is developed on the basis of the modelling equations may be used as a tool for testing of control strategies. Development and testing of control strategies is the subject of a subsequent paper.

1. INTRODUCTION

Availability of a sufficiently accurate macroscopic mathematical model of traffic flow is an important prerequisite for design and testing of modern freeway traffic control strategies. For the Boulevard Périphérique (BP) in Paris, it is intended to develop and investigate traffic responsive on-ramp metering strategies. In this context, a macroscopic traffic flow model (META: Modèle d'Ecoulement du Trafic Autoroutier) developed in a previous study (see Papageorgiou *et al.*, 1989), is applied to the southern part of BP which has a total length of 6 km and includes five on-ramps and six off-ramps. META is based on a model originally proposed by Payne (1971) which was extended in Papageorgiou *et al.* (1989), to consider weaving phenomena at on-ramp locations. In the present paper, a further extension is introduced in order to consider weaving phenomena due to a lane drop. These two extensions prove to be important for an accurate description of complex traffic flow phenomena. Theoretical modelling issues and limitations along with a literature review and comparison with alternative macroscopic models may be found in Papageorgiou *et al.* (1989).

The present paper, which is an extract of the first part of a detailed report by Papageorgiou (1988), concentrates on application and validation of the model on the basis of real traffic data and on development of a simulation program. A subsequent paper describes application of META for design and testing of coordinated, traffic responsive on-ramp metering strategies.

2. DESCRIPTION OF THE SOUTHERN PART OF BOULEVARD PERIPHERIQUE

Geometrical data

A functional sketch of the internal side of the southern part of BP including five on-ramps and six off-ramps is shown in Fig. 1. The total length of the stretch being 5.93 km, a subdivision into 12 sections, each approximately 500 m long, can be effectuated as indicated in Fig. 1. It should be noted that the BP stretch considered by Papageorgiou *et al.* (1989) consists of sections 10 and 11 in Fig. 1.

On-ramp metering facilities exist for the on-ramps Italie, Chatillon, and Bancion. On-ramp metering is effectuated by use of ordinary traffic lights with a traffic cycle of 40 s.

Available measurement information

There are 13 mainstream detector stations located at the boundaries of the 12 sections. These detector stations will be referred to by the number of the upstream section, the very first station being denoted by zero. Each station includes 2 or 3 detectors according to the corresponding number of lanes. Traffic volumes for each on-ramp or off-ramp are measured by corresponding detectors.

Collected data consist of measurements of car passages and occupancies for each detector over a chosen time interval. Using an estimated mean effective vehicle length, mean speed estimates w have been derived for each detector station, see Papageorgiou (1988), for details.

A measurement set is a set of synchronized data

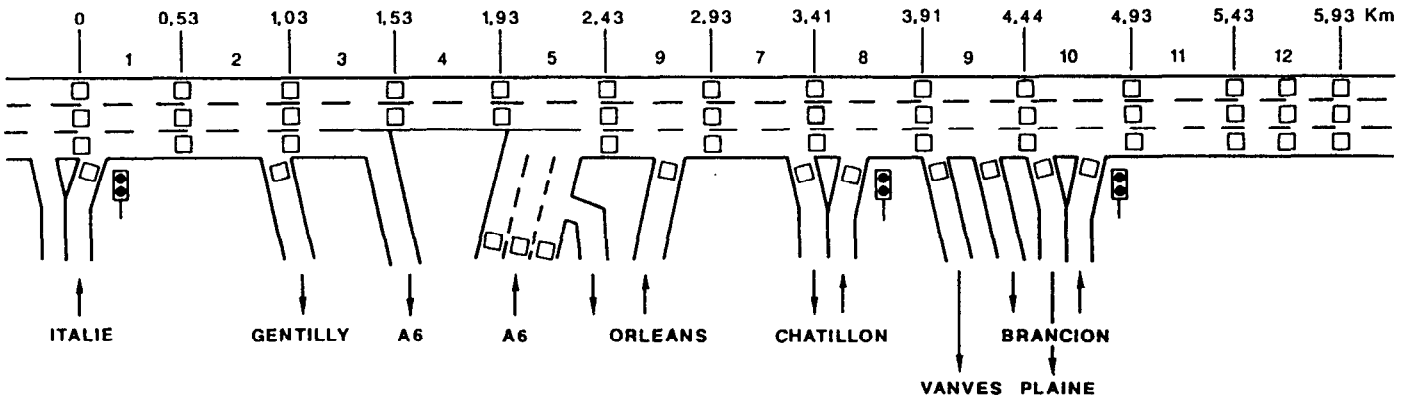

Fig. 1. Functional sketch of the southern part of B.P.

Table 1. Overview of available measurement sets

No.	Date	Time	On-ramp control	Weather	Traffic characterisation
I	27.11.87	6:04–10:04	fixed-time control between 7:00–10:00 h	rainy	heavily congested after 7:40 h
II	02.12.87	6:04–10:04		sunny	congestion after 7:40 h
III	03.12.87	6:00–8:14		sunny	congestion after 7:40 h
IV	09.12.87	11:52–15:52	no	sunny	congested except between 12:50–13:30

collected by the detectors at several system locations over a certain time horizon. Four measurement sets have been available for the present study. Table 1 gives an overview along with a short characterisation of the four measurement sets which include a broad spectrum of traffic conditions (fluid, dense, and congested traffic), of weather conditions, and of times-of-day.

Figure 2 visualises the volume-occupancy diagrams taken over one-minute-intervals for stations 1,6,8 of set I. These diagrams are fairly representative for all measurement sets. Points A,B,C,D in the diagrams of Fig. 2 indicate one, two, three, more than three 1-min-measurements, respectively.

Description of traffic situation

Figure 3 depicts the trajectories of traffic volumes q and mean speeds w (one-minute-data) for the boundary detector stations 0 and 12 for measurement set I.

Typical demands at on-ramps Italie, Chatillon, and Brancion during rush hours exceed 1,000 veh/h. On-ramp Orléans is closed during the period 6:00–8:00 a.m. for safety reasons. Typical demand at the autoroute entrance A6 during rush hours exceeds 3,000 veh/h. Mainstream entrance traffic volume reaches 4,000 veh/h before 7:00 a.m. (Fig. 3a). Off-ramp volume values are around 500 veh/h.

The general traffic situation in the southern part of BP on weekdays is dominated by heavily congested peak hours traffic in the morning (7:00–10:00) and in the evening (16:00–19:00). Figure 3b depicts the breakdown of mean speed at the beginning of the morning peak hours period. Between the two daily peak hour periods, traffic may be oscillating partially strong, partially congested, and partially fluid, the extent of each situation depending upon the particular conditions of the day. The main bottleneck of traffic flow in the considered stretch of BP seems to be due to excessive on-ramp volumes from A6 combined with high mainstream volumes entering the two-lane-stretch (sections 3 and 4). As a consequence of the congestion, A6 entrance volume finally achieves average values around 2,500 veh/h which is clearly below demand and causes a queue of several kilometers on A6. Furthermore, mainstream traffic through stations 3 and 4 reduces to values below 2,500 veh/h whereas mean speeds in sections 1–4 reach values of 15 km/h or less. This typical situation is visualized on the basis of traffic volume distribution in Fig. 4. As far as sections 5–12 are concerned, the spatial distribution of mean speed during peak hours is typically increasing, passing from 30 km/h at station 6, to 64 km/h at the stretches exit. The spatially averaged speed along the BP stretch for the traffic situation of Fig. 4 amounts to 35 km/h.

A further bottleneck is known to exist downstream of the considered stretch. When this latter bottleneck causes congestion, traffic of the considered BP stretch may be affected, namely if this congestion mounting in upstream direction reaches station 12. This situation can be observed in Fig. 3b at about 8:00 a.m.: Congestion mounting from downstream leads to strong oscillations (10–50 km/h) of mean speed at station 12, exit traffic volume reducing to 4,000 veh/h in the average. When this type of bottleneck occurs, congestion becomes even more severe in the first half of the BP stretch, mean speeds being further reduced to 10 km/h or less.

Figure 5 shows traffic volumes distribution during this type of severe congestion. Exit rates in Fig. 5 are higher than in Fig. 4 probably due to diversion caused by severe congestion. The spatially averaged speed in the considered BP stretch during traffic conditions of Fig. 5 amounts to 20 km/h.

Some of the characteristics of the described traffic situation on the considered BP stretch are reflected on the fundamental diagrams depicted in Fig. 2:

(i) Due to the sudden breakdown of mean speed at 7:00 a.m., a discontinuity appears on the diagrams of stations 0–6 whereas no discontinuity is visible on the diagrams of sections 7–12.
(ii) Maximum traffic volumes at the three-lane-station 1, observed in Fig. 2a, hardly exceed 5,500 veh/h although stations 6 and 8 having a similar geometry, experience maximum volumes of 6,300 veh/h and more. This is due to the bottleneck occurring in sections 3 and 4 which does not permit traffic volumes of stations 0 and 1 to reach capacity values.

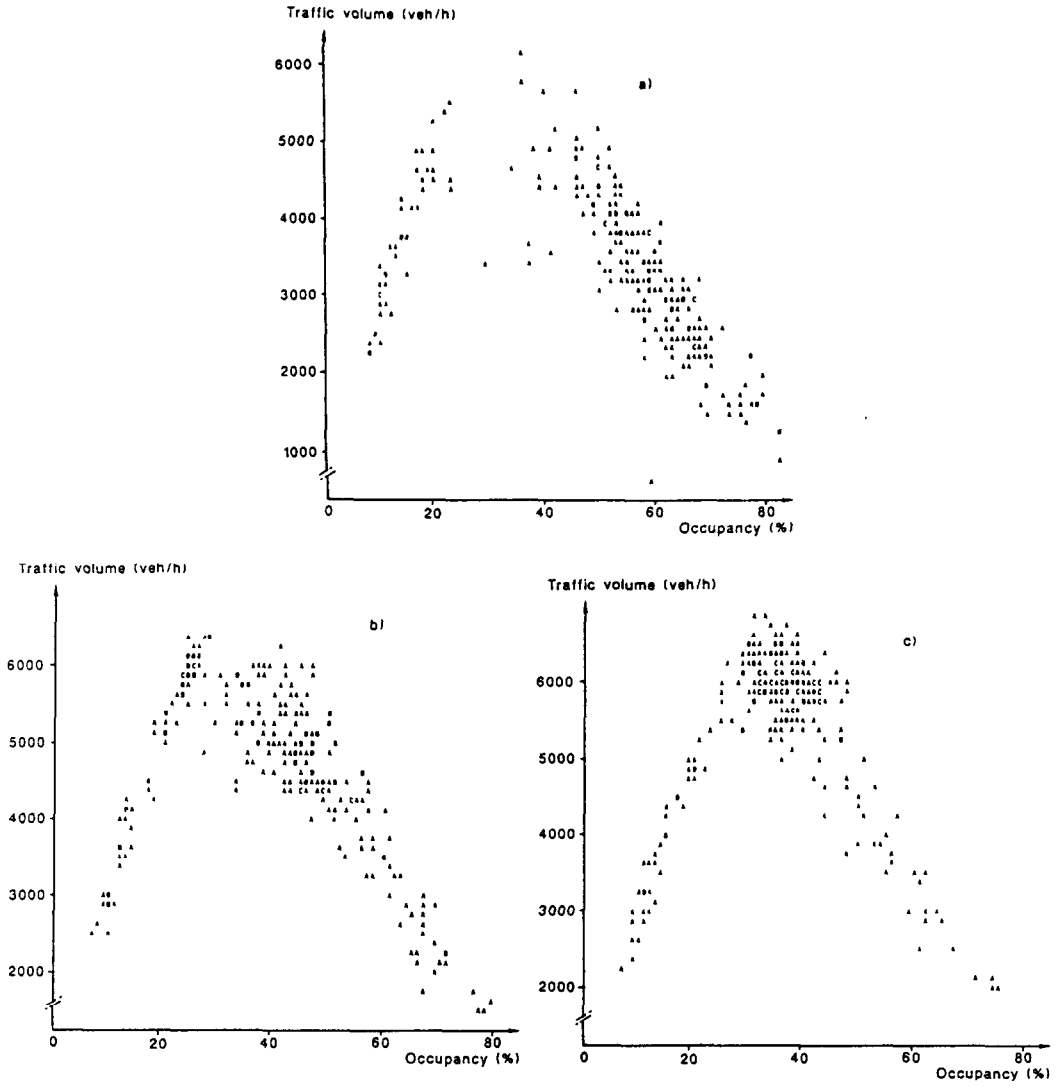

Fig. 2. Volume-occupancy diagrams Set I, Stations 1(a), 6(b), 8(c).

3. MODELLING OF TRAFFIC FLOW ON THE SOUTHERN PART OF BOULEVARD PERIPHERIQUE

Basic modelling equations

Macroscopic description of traffic flow implies the definition of adequate flow variables expressing the average behaviour of the vehicles in a given freeway section i. For a space/time-discretized presentation, we define traffic density $\rho_i(k)$ as the number of cars in the section at time $t = kT$ divided by the section length Δ_i where $k = 0,1,2, \ldots$ is the discrete time index, and T denotes the sample time interval. Similarly, we define mean speed $v_i(k)$ as the mean speed of the cars included in the section at time $t = kT$. Finally, $q_i(k)$ is the number of cars leaving the section during $kT < t < (k + 1) \cdot T$, divided by T. On-ramp and off-ramp volumes $r_i(k)$ and $s_i(k)$ are defined in an analogous way.

The macroscopic traffic flow model D described in Papageorgiou *et al.* (1989), (see therein for a theoretical discussion and a more comprehensive literature review) consists of the following equations applying to each section of a given freeway:

$$\rho_i(k+1) = \rho_i(k) + \frac{T}{\Delta_i}[q_{i-1}(k) - q_i(k) + r_i(k) - s_i(k)] \tag{1}$$

$$q_i(k) = \rho_i(k)\, v_i(k) \tag{2}$$

$$v_i(k+1) = v_i(k) + \frac{T}{\tau}[V(\rho_i(k)) - v_i(k)] + \frac{T}{\Delta_i} v_i(k)[v_{i-1}(k) - v_i(k)] - \frac{\nu T}{\tau \Delta_i} \frac{\rho_{i+1}(k)/\lambda_{i+1} - \rho_i(k)/\lambda_i}{\rho_i(k)/\lambda_i + K} - \frac{\delta T}{\Delta_i} \frac{r_i(k) v_i(k)}{\rho_i(k) + K\lambda_i} \tag{3}$$

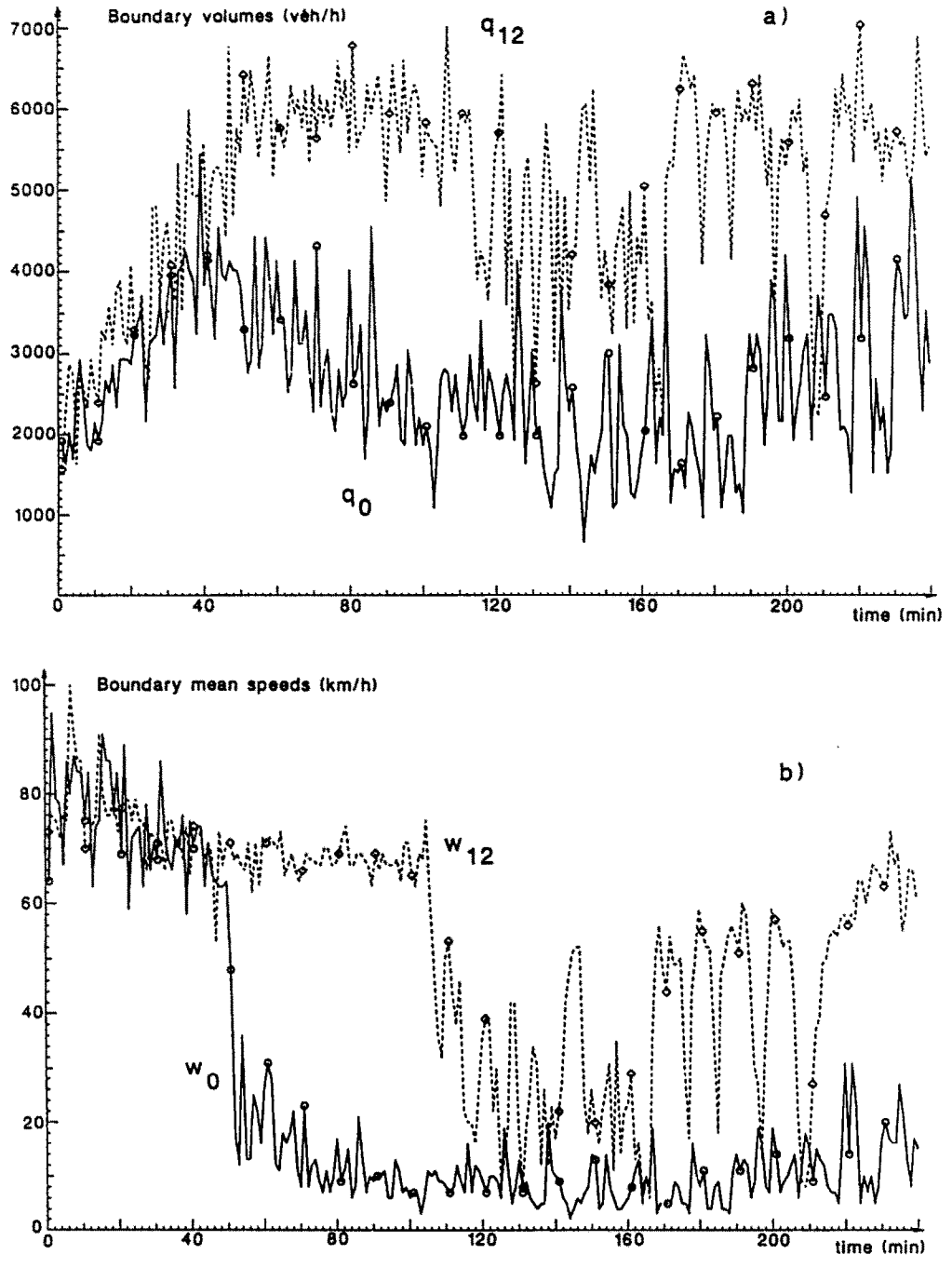

Fig. 3. Boundary trajectories of measurement set I traffic volume (a), mean speed (b).

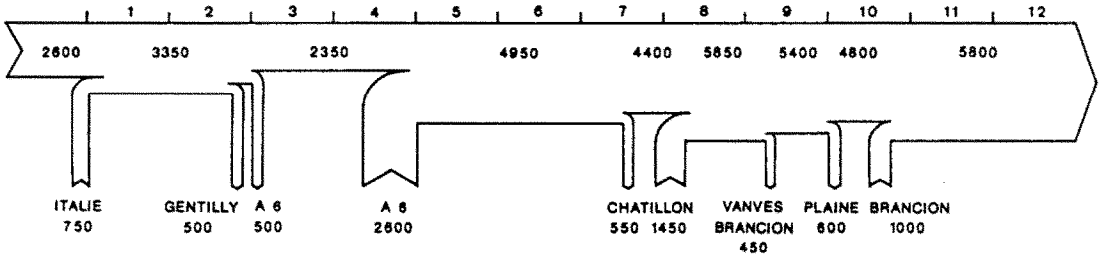

Fig. 4. Typical traffic volumes without exit blocking (measurement sets II, III).

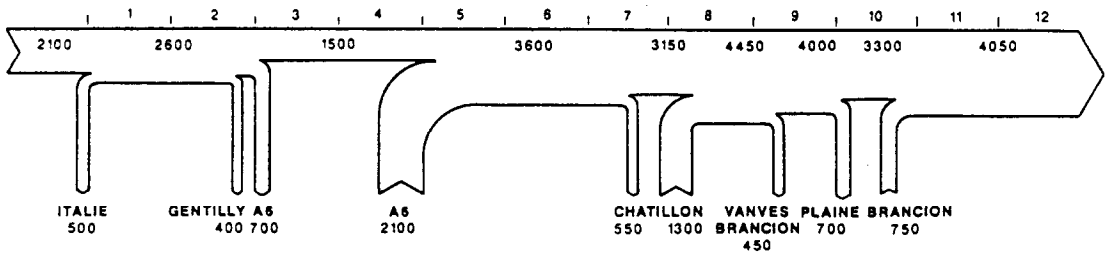

Fig. 5. Typical traffic volumes with exit blocking (measurement set I).

$$V(\rho_i) = v_f \exp\left[-0.5\left(\frac{\rho_i}{\lambda_i \cdot \rho_{cr}}\right)^2\right] \qquad (4)$$

with the constant parameters v_f (free speed), ρ_{cr} (critical density per lane), τ (time constant), ν (anticipation constant), and δ (on-ramp constant). Parameter K is chosen equal to 13 veh/km. λ_i denotes the number of lanes in section i. Equation (1) is the well-known conservation equation. Equation (2) results from its analogon in Papageorgiou *et al.* (1989), by setting a parameter $\alpha = 1$. In fact, $\alpha < 1$ does not lead to a significant amelioration of model accuracy. For the same reason, the parameter ζ introduced by Papageorgiou *et al.* (1989) in the third term (convection term) of the right-hand side of (3) is set equal to unity. Equation (3) is a dynamic speed-density relationship whilst (4) is a static, monotonically decreasing function utilized in the second term of the right-hand side of (3). Combining (2) and (4), one obtains a function $Q(\rho_i) = \rho_i \cdot V(\rho_i)$ which is broadly known as the fundamental diagram of traffic engineering. One can easily show that $Q_{\max} = Q(\lambda_i \rho_{cr})$, (i.e. traffic flow) obtains its maximum value for $\rho = \lambda_i \rho_{cr}$.

Mean speed resulting from (3) is limited by, say, $v_{\min}$ (e.g. $v_{\min} = 1$ km/h). Mean speed w_i at the boundary between section i and $i + 1$ is supposed to be equal to v_i, the mean speed of the upstream section i. (This is a consequence of the assumption $\alpha = 1$.)

The presented macroscopic traffic flow model is based on a model originally proposed by Payne (1971). It was reported in the literature (see e.g. Cremer and May, 1986) that Payne's model may have poor performance in case of a lane drop. In fact, drivers traveling on the lane(s) to be dropped are forced to change lane and this may cause a reduction of mean speed in the section immediately upstream of the lane drop site. Obviously, this cause of speed reduction is not considered in (3).

Lane changing due to a lane drop may be understood as a phenomenon which is similar to on-ramp traffic injection into the mainstream. Eventually, an additional term in (3) may preserve the structure of the last term of the right-hand side of (3). In this case, r_i should be replaced by the lane changing traffic volume which is roughly equal to $q_i(\lambda_i - \lambda_{i+1})/\lambda_i$ with $\lambda_{i+1} < \lambda_i$. But if q_i is substituted using (2), we obtain the additional term $-\phi T/\Delta_i \cdot (\lambda_i - \lambda_{i+1})/\lambda_i \cdot v_i(k)^2$, where ϕ is a new constant parameter. It is interesting to note that a similar term appears in modelling of unsteady water flow in open channels. Of course, speed reduction due to lane drop is expected to be more pronounced for dense or congested traffic, for which reason the additional term was finally modified as follows.

$$-\phi T/\Delta_i \cdot (\lambda_i - \lambda_{i+1})/\lambda_i \cdot \rho_i(k)/(\rho_{cr} \cdot \lambda_i) \cdot v_i(k)^2. \qquad (5)$$

This term is added to the right-hand side of (3) whenever $\lambda_{i+1} < \lambda_i$. In the present application, this term is uniquely applied to section 2 since there is a lane drop from section 2 to section 3 (the right lane of section 3 is exclusively used by cars exiting to A6).

Model application to the southern part of Boulevard Périphérique

Application of the macroscopic model to the southern part of BP is based on a subdivision into 12 sections as presented in Fig. 1. The time interval T is chosen to be 10 s so as to respect the inequality $T < \Delta/v_f$.

For parameter estimation and model validation, it is necessary to distinguish input variables from output variables in the measurement data. As explained in Papageorgiou *et al.* (1989), input variables are the boundary variables of stations 0 and 12 as well as the on-ramp and off-ramp volumes. The model being fed with these measured data, traffic volumes, and mean speeds for the internal measurement sites, as produced by the model equations, may serve as output variables to be compared to the corresponding real traffic data. Details of model application to the considered BP-stretch are given in Papageorgiou (1988).

The same parameter δ is used in the mean speed eqn (3) for all sections including an on-ramp in spite of existing differences of the ramps' geometry. Merely for the on-ramp A6, r_5 is replaced by max $(0, r_5 - 2000)$ in the last term of the right-hand side of (3). This is necessary because the shoulder lane of section 5 is exclusively dedicated to entering traffic. Hence, considerable weaving phenomena justifying the on-ramp deceleration term in (3), are expected only if entering traffic exceeds capacity of the shoulder lane which is roughly equal to 2,000 veh/h.

In spite of the different shapes of the fundamental diagrams appearing in Fig. 2 at different sites, the same parameters v_f, ρ_{cr} are used for all sections. In other words, the static function (4) is only dependent

upon the number of lanes λ_i of a given section. The different shapes observed in Fig. 2 for sections with equal number of lanes must therefore be described by the dynamic portion of the model.

4. PARAMETER ESTIMATION

Nominal parameter values

There are six model parameters to be estimated: v_f, ρ_{cr}, τ, ν, δ, ϕ. Parameter values should be specified so as to minimize the deviation of the model's output (i.e. mean speeds and traffic volumes of all internal sites) from the corresponding measured values. The parameter estimation problem is thus transformed into an optimization problem which may be resolved for each available measurement set. An extensive discussion on the optimization problem characteristics and on appropriate solution algorithms may be found in Cremer and Papageorgiou (1981), and in Papageorgiou (1983).

The estimated parameters resulting from optimization may be different for each measurement set but it is not difficult to specify a nominal set of parameter values which performs satisfactorily for all measurement sets. This nominal set reads

$$v_f = 90 \text{ km/h}; \rho_{cr} = 37.3 \text{ veh/km/lane}; \tau = 36 \text{ s};$$
$$\nu = 35 \text{ km}^2\text{/h}; \delta = 0.8; \phi = 2.$$

Free speed v_f being equal to the one estimated in Papageorgiou *et al.* (1989), the maximum traffic volume Q_{max} in the fundamental diagram of a three-lane-section is slightly reduced to $Q_{max} = 6{,}114$ veh/h due to an according reduction of the estimated critical density ρ_{cr}. Again it should be underlined that the same parameter values v_f, ρ_{cr} are used for all sections in spite of the different shapes of the fundamental diagram appearing at different sites in Fig. 2.

The modifications of τ and ν as compared to the values found in Papageorgiou *et al.* (1989) were necessary to a certain degree in order to compensate the simplifications $\alpha = \zeta = 1$. On the other hand, the changed time/space discretization intervals may also be at the origin of these modifications.

In contrast to the results in Papageorgiou *et al.* (1989), the parameter δ obtains a fairly high value in the present study. Actually, reduction of mean speed due to high on-ramp volumes proves to be a non-negligible phenomenon of traffic flow on Boulevard Périphérique, and the available data material of this study permits an estimation of its importance as reflected in the value of δ.

Although parameter ϕ attains a relatively high value, its importance in terms of quantitative accuracy is moderate. In fact, the main contribution of the corresponding term in (3) is a more accurate description of the spatial distribution of mean speed in the first four sections. More precisely, measured mean speed at station 2 is usually slightly lower than mean speed at stations 1, 3, 4. This relation is not reproduced by the model if $\phi = 0$. Naturally the value of ϕ may generally depend upon the particular geometry of a lane drop site.

Performance criterion values

Reliability of the model is underlined by the fact that performance variations with respect to different stations, and measurement sets were found to be rather moderate. The general averages over all sites and all measurement sets of traffic volume standard deviation (714 veh/h) and mean speed standard deviation (10.8 km/h) are very satisfactory.

Output trajectories

Some output trajectories are shown in Figs. 6–9 (solid lines depict measured trajectories whilst dashed lines depict the corresponding model outputs). The morning breakdown of mean speed occurring in the measurement sets I, II, III is reproduced fairly accurately by the model (see e.g. Fig. 6). Congestion mounting from downstream and reaching station 12 is propagated by the model in upstream direction with considerable accuracy (see detailed results in Papageorgiou (1988)).

An intermediate fluidity period of less than one hour included in measurement set IV, is reproduced fairly well by the model (see Fig. 7). The worst result with respect to mean speed, which was achieved for station 3 of measurement set IV, is shown in Fig. 8. Clearly the corresponding standard deviation of 20.1 km/h is due to excessive stop-and-go conditions which are less pronounced in the model results.

With respect to traffic volumes, measured trajectories are followed fairly accurately by the model trajectories both for fluid traffic and for congested traffic. Figure 9 depicts the worst result with respect to traffic volume, which was achieved for station 1 of measurement set IV. Again, description of traffic volume by the model equations appears satisfactory.

5. SENSITIVITY INVESTIGATIONS

Sensitivity investigations in the present chapter follow the lines of Papageorgiou *et al.* (1989, Chapter 5). First a quantity

$$\delta J(\beta) = J(\beta) - J(\beta^*) \tag{6}$$

is defined where $J = J_w + 0.01\, J_Q$, and J_w, J_Q are the averaged (over all internal stations) error standard deviations of the output trajectories with respect to mean speed and traffic volume respectively. β^* is the vector of nominal parameters. Figure 10 depicts sensivity diagrams obtained by changing one parameter at a time in the range

$$-0.6 < (\beta_i - \beta_i^*)/\beta_i^* < 0.5$$

whilst all other parameters are kept equal to their nominal values. Each diagram depicts this parameter

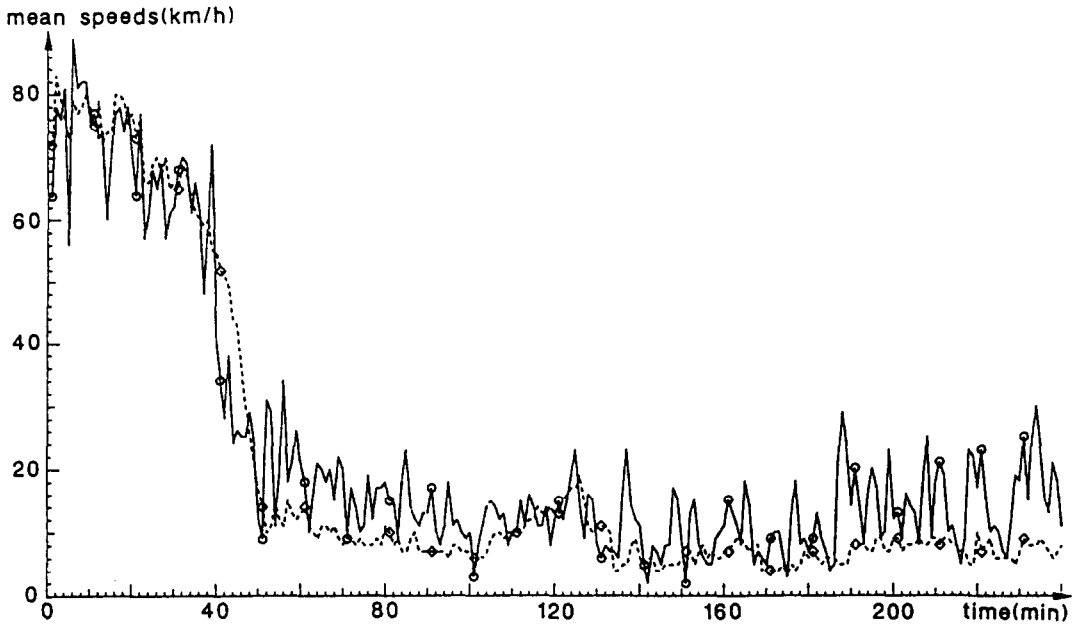

Fig. 6. Mean speed for measurement set I, station 2.

change ratio versus the corresponding performance change ratio $\delta J/J^*$ for each of the four available measurement sets. Sensitivity of parameter τ is investigated by modifying its values only in the second term of the right-hand side of (3).

Free speed v_f and critical density ρ_{cr} are seen to be the most sensitive parameters, a phenomenon which was also observed in analogous investigations by Papageorgiou *et al.* (1989) and by Cremer and Papageorgiou (1981). In the present study, sensitivity of these parameters appears even higher for the following reason: the most important event to be described by the model in the present application is occurrence and dissipation of congestion in sections 1–4. It is well known that during congestion, traffic waves propagate in upstream direction. Thus, congestion in sections 1–4 is not visible at the stretches exit (station 12) and consequently the model is required to describe occurrence and dissipation of congestion only on the basis of the input information at the stretches entry (station 0), the on-ramps, and the off-ramps. Typically, measured volume q_0 increases steadily after 6:00 a.m. until a congestion occurs. Assume that for a non-nominal parameter set, the model has not yet created a congestion at the moment this congestion occurs in real life. In this case, measured volume q_0

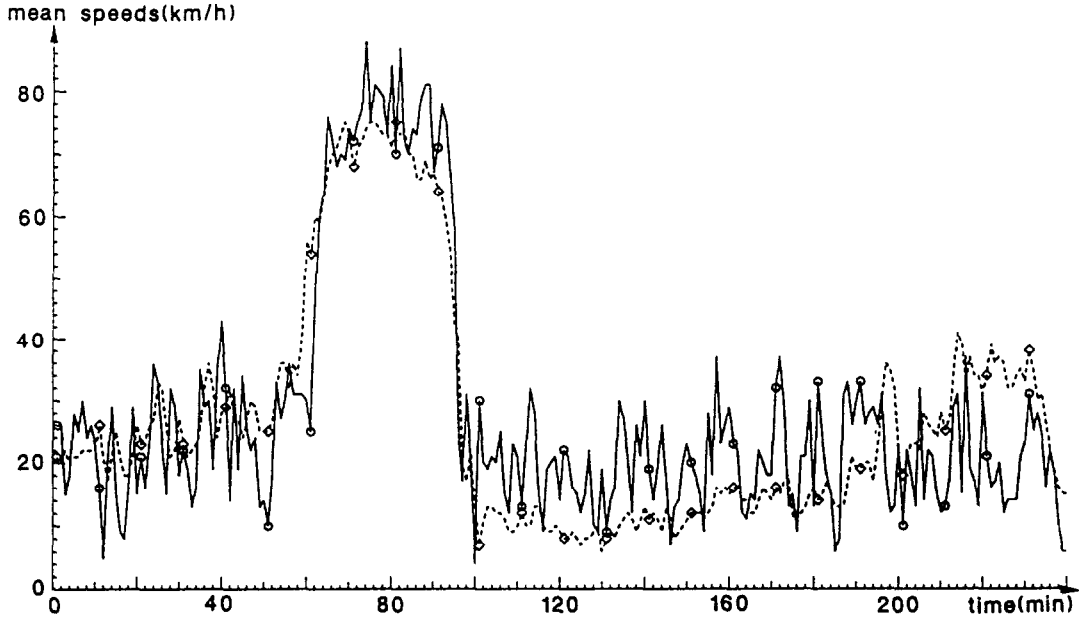

Fig. 7. Mean speed for measurement set IV, station 1.

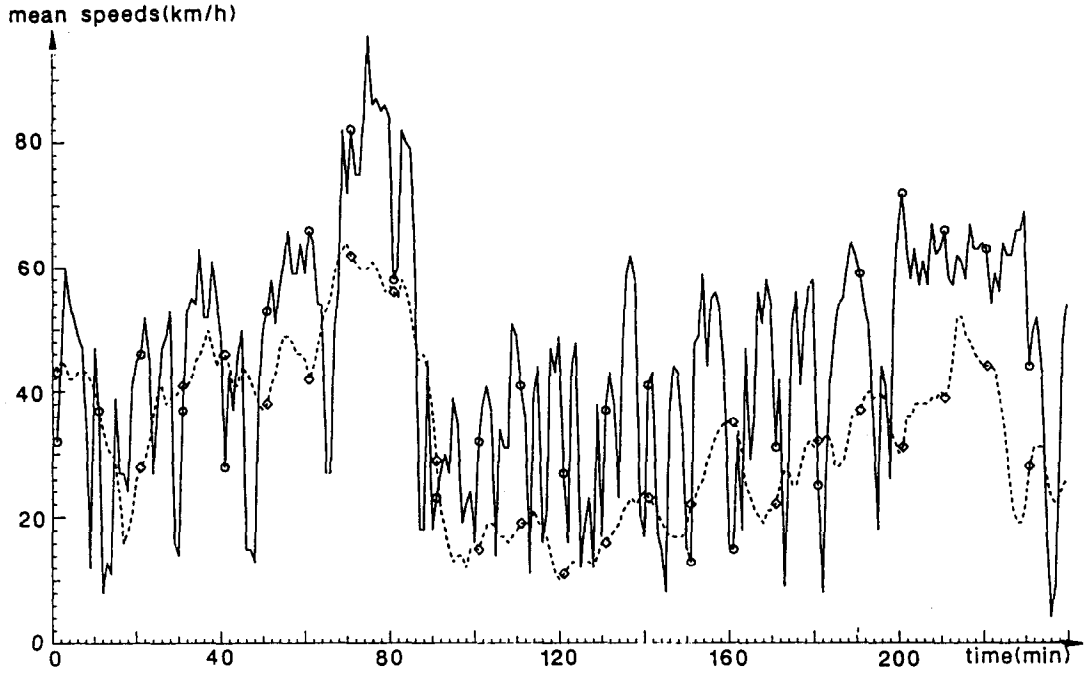

Fig. 8. Mean speed for measurement set IV, station 3.

which was steadily increasing before congestion, will be reduced due to the occurrence of congestion. But since model equations are still fed with q_0 which is now low, it may happen that the congestion will never be created by the model. Clearly the real sensitivity of the model is much less than reflected by this particular situation. In fact, if the mainstream demand, further upstream of station 0, instead of q_0, were known, congestion might have been reproduced later than in real-life even with non-nominal parameters. An analogous reasoning applies during congestion dissipation. We may therefore conclude that the sensitivity results of Fig. 10 are feignedly amplified due to the particular application conditions. In fact, if

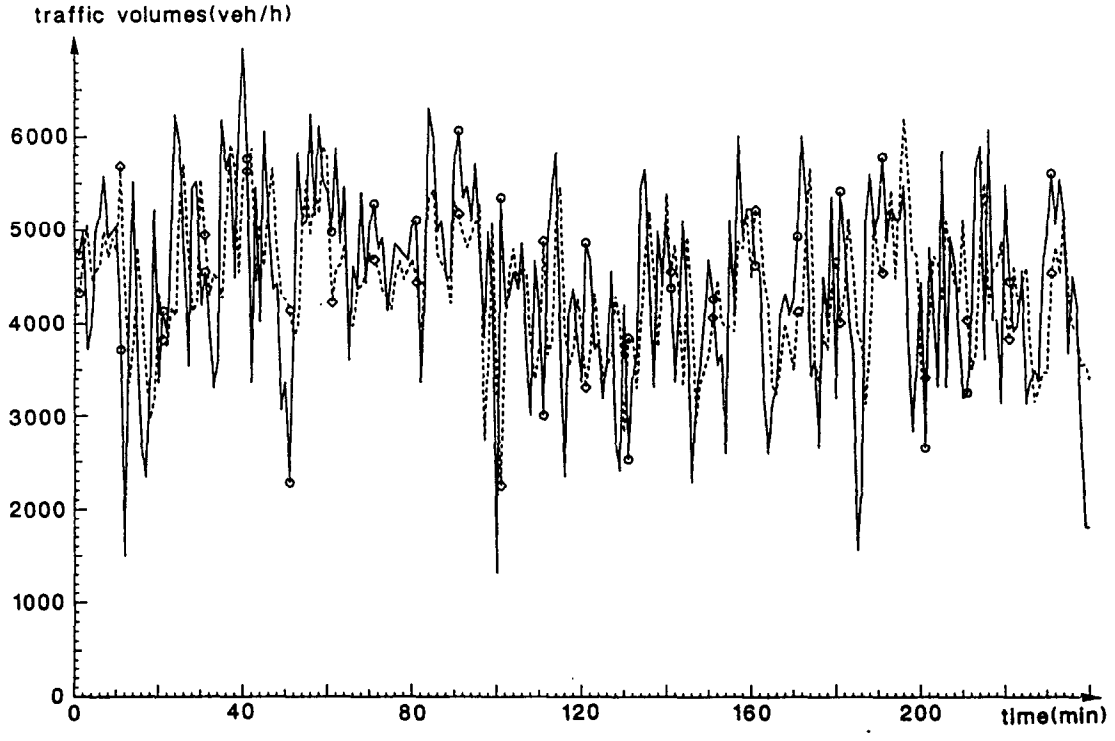

Fig. 9. Traffic volume for measurement set IV, station 1.

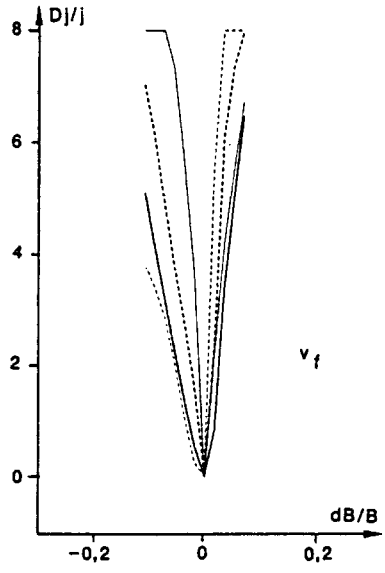

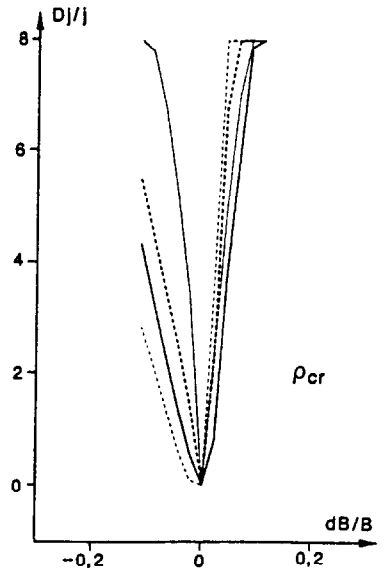

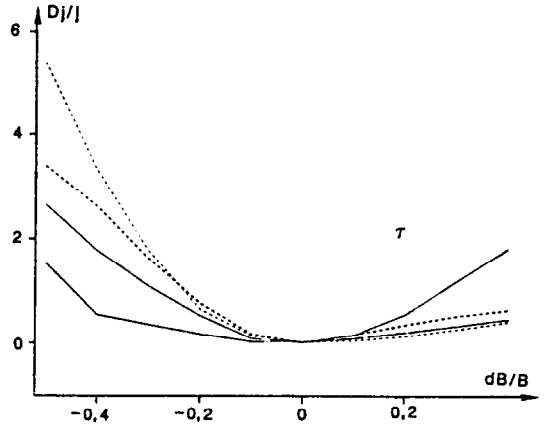

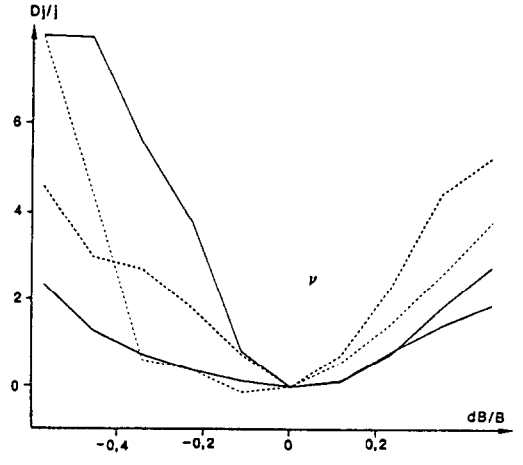

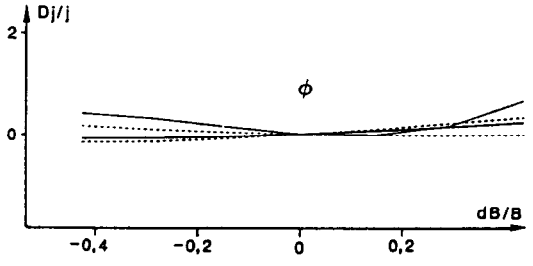

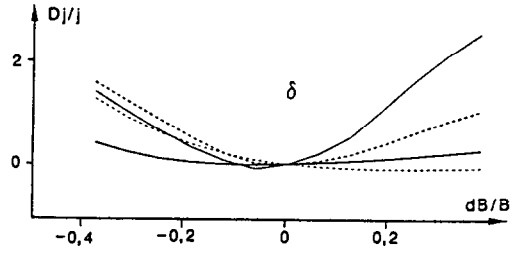

Fig. 10. Sensivity diagrams.

model equations are fed with $q_0 = q_0^m \cdot (v_1/v^m_0)$ instead of $q_0 = q_0^m$ (upper index m denoting measured values) where v_1 is the modelled mean speed for section 1, the values of the resulting performance criterion J are only slightly changed but the resulting sensitivity diagrams change dramatically as indicated by Fig. 11.

This modified utilisation of upstream boundary measurements may be interpreted in the following way: a buffer section 0 is introduced with density $\rho_0 = q^m_0/v^m_0$ and mean speed $v_0 = v_1$. It should be noted that above modification should be actually introduced under similar application conditions if the model is to be utilized for traffic data reconstruction (estimation) between two detector stations in a real-time environment.

A further phenomenon which is worthwhile to mention, is the existence of what might be called "diagonal valleys" of the performance criterion J in the parameter space. This is to say that the deterioration of J caused by modification of one parameter may be partially compensated by suitable modification of one or more other parameters. This provides a certain flexibility in the choice of parameter values and of model structure, but is probably an indication of poor identifiability of some parameters (see also Grewal and Payne, (1976)). With respect to parameters τ, ν, δ, ϕ model sensitivity is seen in Fig. 10 to be rather low.

In what concerns the sample time interval T, model results were found to be practically identical for $T = 5$ s, 10 s, 15 s, a dramatic deterioration appearing – probably due to numerical instability – for $T = 20$ s.

6. A SIMULATION PROGRAM

The macroscopic model developed in the previous chapters may be used as the kernel of a simulation program for the traffic flow on the southern part of BP aiming at testing and comparing the efficacy of different control strategies. For the development of the simulation program some organizational and modelling questions must be accomplished. The simulation program should be able to describe any real or hypothetical traffic situation. In the latter case, on-ramp demand and boundary conditions must be specified by the user.

Upstream boundary

Mean speed values v_0 needed in (3) for section 1 are set equal to v_1. If density ρ_1 is overcritical, mainstream volume q_0 is limited to $Q(\rho_1)$ (i.e. to the value of the fundamental diagram corresponding to ρ_1). In this case, a mainstream queue l_0 (veh) is assumed to be formed

$$l_0(k+1) = l_0(k) + T[q_{0d}(k) - q_0(k)] \qquad (7)$$

where q_{0d} is the given mainstream demand. If a queue l_0 is present, the amount of mainstream volume wishing to enter is augmented to $q_{0d}(k) + l_0(k)/T$ but the final mainstream volume $q_0(k)$ is not allowed to exceed $Q(\lambda_l \cdot \rho_{cr})$, the maximum traffic volume of the fundamental diagram.

Downstream boundary

Density ρ_{13} needed in (3) for section 12 is set equal to ρ_{12} unless ρ_{12} becomes overcritical in which case ρ_{13} is set equal to the critical density. In other words, traffic conditions downstream of the considered stretch are generally assumed to be noncongested. If the user wishes to simulate a downstream bottleneck, he may do so by limiting exit volume q_{12} to q_{BOUND}, where q_{BOUND} may be specified by the user.

On-ramp volumes

On-ramp volumes are either set equal to the ramp demand or are specified by a control strategy. After this, on-ramp volumes are limited to a maximum value $r_{i,m}$ which depends upon the ramp geometry and the mainstream density. Figure 12 shows measured on-ramp volumes at A6 and Brancion versus mainstream occupancy o_i measured immediately downstream of the on-ramp. Points of the diagrams have been traced only if measured on-ramp occupancy was higher than 25%, (i.e. only if on-ramp demand was sufficiently high). Under these conditions, the diagrams of Fig. 12 may be understood as $r_{i,m}(o_i)$-relationships for the corresponding on-ramps. Approximating this relationship by the solid lines in Fig. 12 and assuming occupancy to be proportional to density, a function $r_{i,m}(\rho_i)$ may be established. In this way, volumes of each on-ramp are limited according to the mainstream density.

If r_i resulting from above limiting procedure, is less than the demand d_i, a queue l_i (veh) will be formed

$$l_i(k+1) = l_i(k) + T[d_i(k) - r_i(k)]. \qquad (8)$$

Note that a queue may be formed even in the uncontrolled on-ramps due to the described on-ramp volume limitation. Hence, the on-ramp volumes being present at uncontrolled on-ramps before limitation are $d_i(k) + l_i(k)/T$. This value represents at the same time a lower limit for the controllable on-ramp volumes, else a negative queue would result from (8).

Off-ramp volumes

Off-ramp volumes are modelled as constant fractions (exit rates) of mainstream volumes. The values of the exit rates are selected by the user according to what is observed in the measurement material.

Criteria

Comparison of efficacy of different control strategies requires calculation of several criteria such as (see Papageorgiou, 1983): total travel time (veh.h),

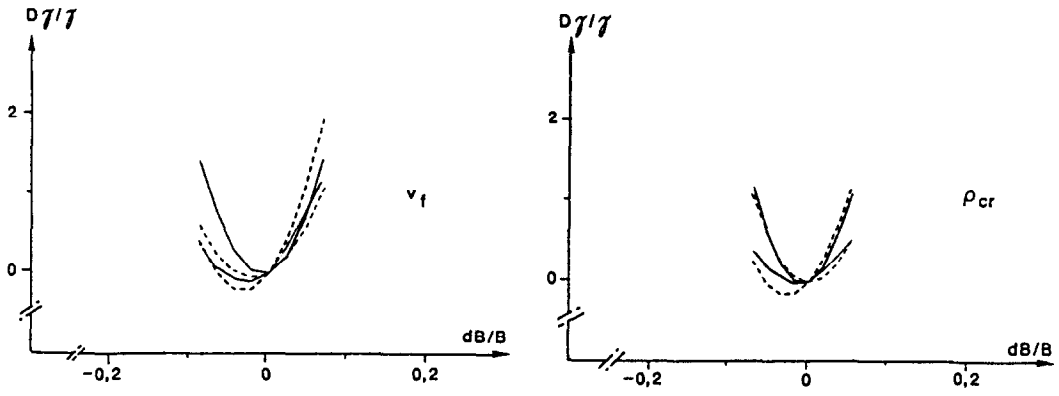

Fig. 11. Modified sensitivity diagrams.

total waiting time at the on-ramps (veh.h), total time spent (veh.h), total travel distance (veh.km), total input (veh), total output (veh), current passing time (min), mean passing time (min), and fuel consumption (veh.l).

A simulation test

The described simulation program was tested under no control conditions using typical morning demand values. Between 6:30–7:30 a.m., demand increases as in real-life. After 8:00 a.m. a congestion is supposed to mount from downstream which blocks the exit of the stretch in a similar way as already observed in measurement set I. Figure 13 depicts the simulated on-ramp volume, mainstream volume, and traffic density trajectories in section 5. It may be seen that the mainstream steady-state situation during the period $80 \leq t \leq 120$ corresponds to the situation of Fig. 4. After exit blocking becomes active, a congestion mounts in the simulated BP-stretch and the mainstream traffic situation around $t = 140$ becomes very similar to the real-life situation of Fig. 5.

Naturally, excessive stop-and-go conditions observed in the real-life trajectories are not reproduced

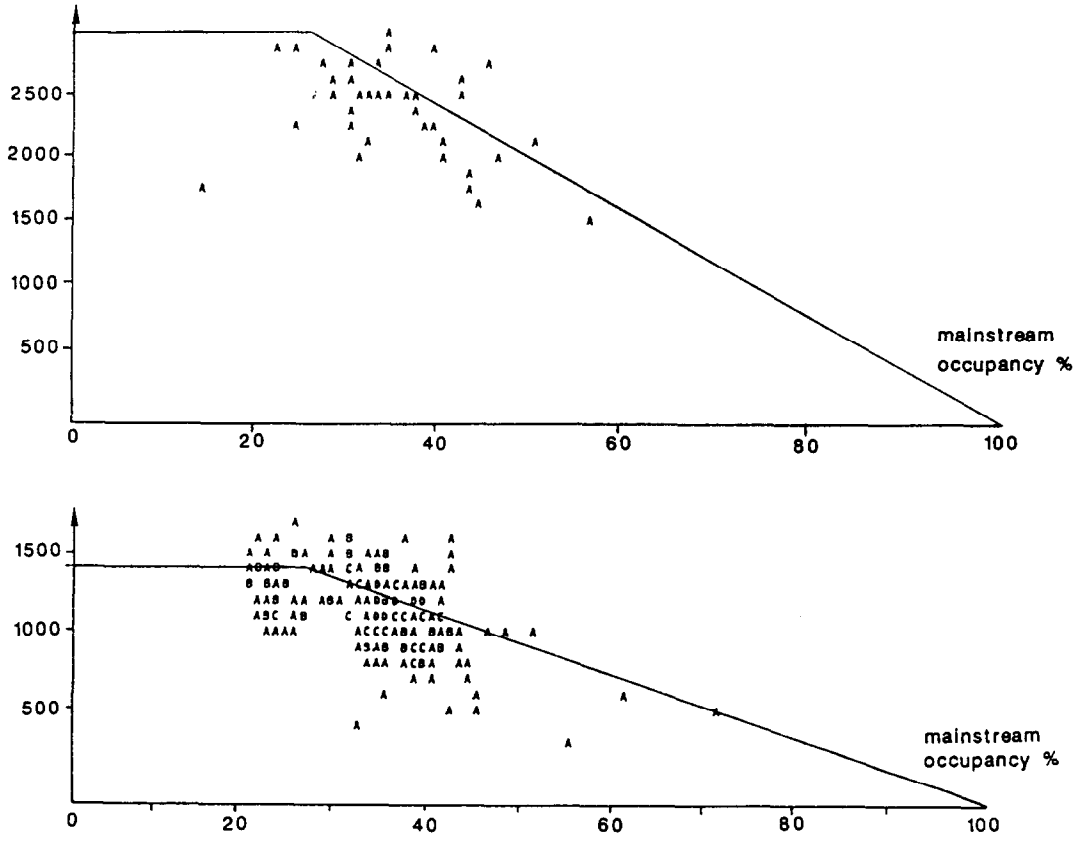

Fig. 12. Maximum on-ramp volumes vs. mainstream occupancy for A6 (a) and Brancion (b).

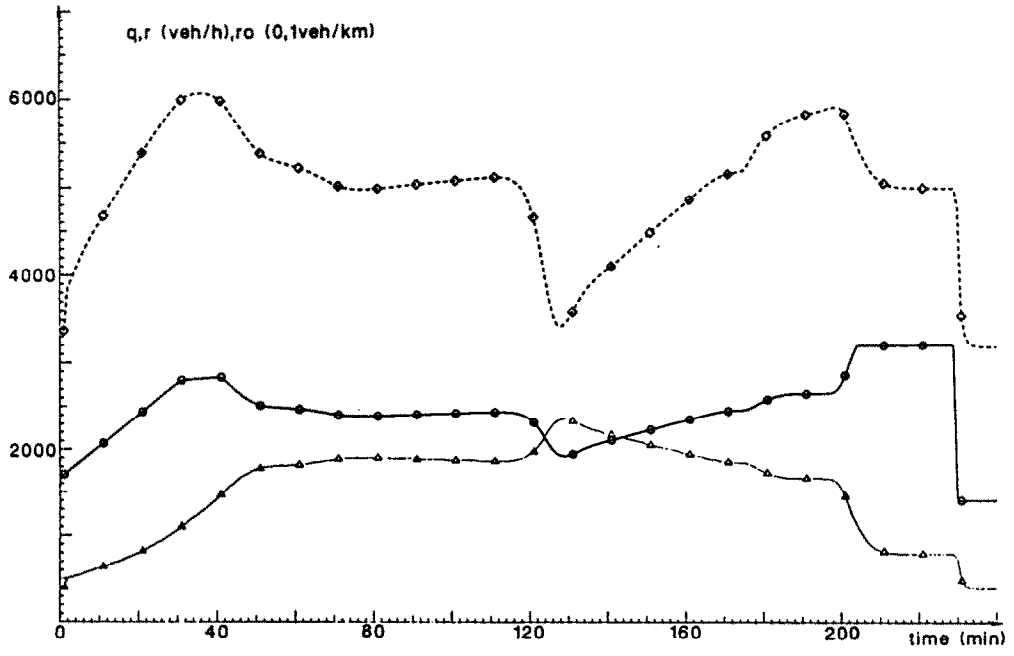

Fig. 13. Results of simulation test for section 5.

by the deterministic traffic flow model fed with deterministic inflows. After 8:30 a.m., demand is artificially reduced in order to obtain free flow conditions at the end of the simulation period, Figure 14 depicts the volume-density diagrams of sections 1,6,8 obtained by using one-minute simulation data. The diagrams give rise to the following remarks:

(i) Critical densities are higher at sections 5,8,10 which contain an on-ramp, a phenomenon which was observed in the real traffic data in Papageorgiou *et al.* (1989). On the contrary, at section 1, which also containts an on-ramp, critical density does not seem to be higher than in sections without on-ramp, but this is consistent with the corresponding real-life diagram of Fig. 2 and is probably due to the influence of the bottleneck in sections 3,4.

(ii) The maximum volumes appearing in the diagrams may differ even though the corresponding sections have the same number of lanes. In particular, maximum volume in section 1 does not exceed 5,000 veh/h which is in accordance with real data of Fig. 2.

(iii) Although a visual discontinuity is not apparent in the simulation diagrams, we know from Figs. 6–7 that mean speed reduces abruptly when a congestion is created.

(iv) Diagrams of Fig. 14 are subject to some hysteresis phenomena which have also been observed in real life (see e.g. Treiterer and Meyers, 1974; Hall and Gunter, 1985).

An important conclusion may be drawn from above remarks and from the fact that the same static volume-density relationship was used for all freeway sections: the discontinuities or hysteresis phenomena in different diagram shapes (in particular different maximum volumes or critical densities) which are observed in the simulation data, are a consequence of the dynamic portion of the modelling equations rather than of the fundamental diagram itself. This indicates that similar phenomena observed in real-life, may only be explained on the basis of the spatial and temporal distribution of traffic flow rather than on the basis of spatially limited observations such as the fundamental diagram.

7. APPLICATION AREAS

The developed mathematical model of traffic flow has been called META (Modèle d'Ecoulement du Trafic Autoroutier). The modelling equations of META are used in a following paper for derivation of coordinated control strategies. Furthermore, META is utilised in the form of a simulation program for validation and comparison of control strategies.

There are, however, further possible application areas of META which include:

(i) On-line reconstruction of real traffic data between two distant (e.g. 3 km or more) detector stations. This application is particularly attractive for sparsely equipped freeway systems. The modelling equations being fed with measured boundary measurements†, full information about the internal traffic state may be furnished by META in real time.

(ii) On-line prevision of traffic flow based on previ-

†Boundary measurement are supposed to include traffic volumes (or demands) at all internal on-ramps and off-ramps.

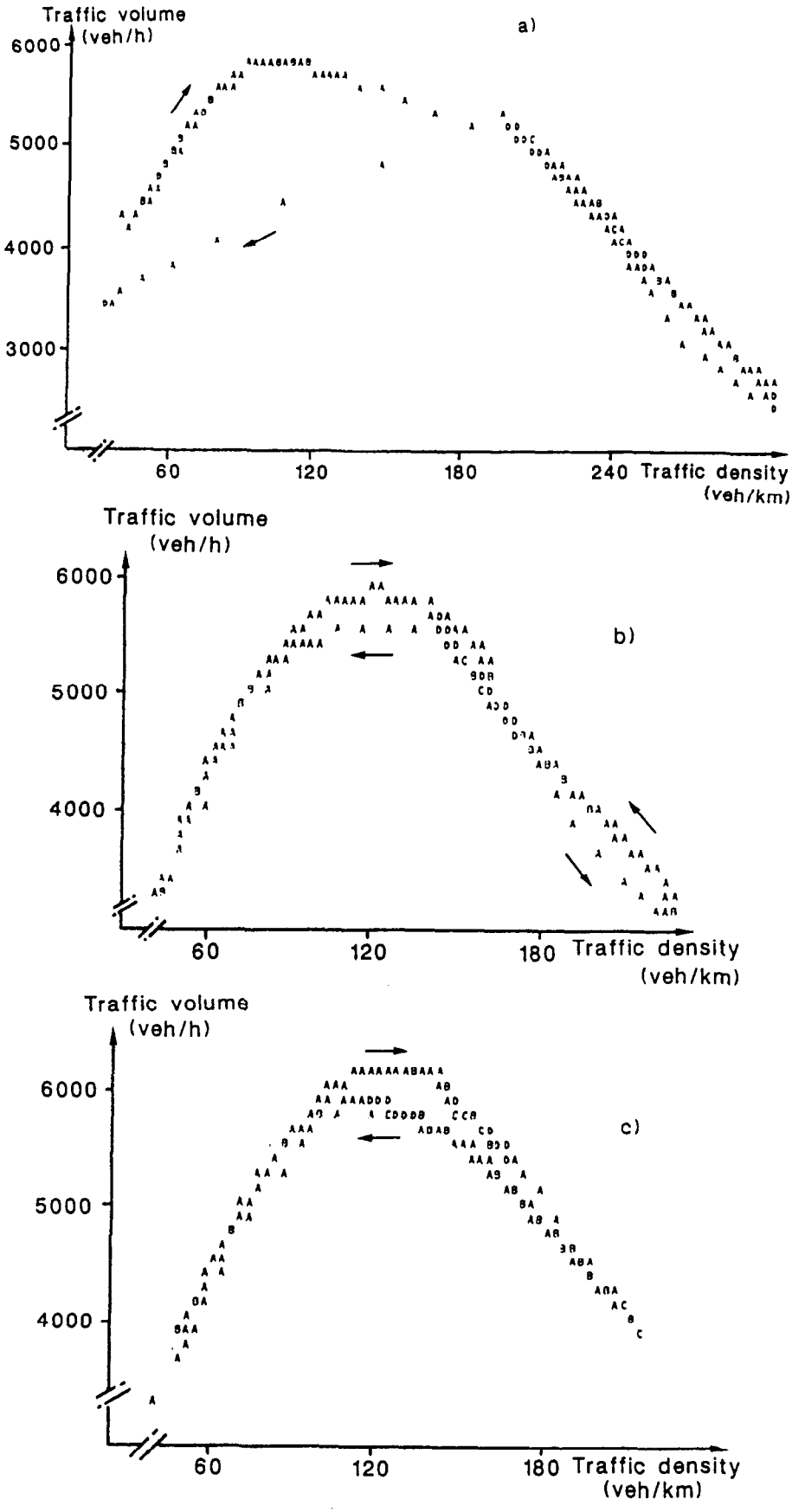

Fig. 14. Fundamental diagrams for simulated data section: 1(a); 6(b); 8(c).

sion of the boundary values needed in the modelling equations.

(iii) Analysis and simulation of traffic conditions based on historical or hypothetical boundary values.

Clearly, these tasks can also be performed under changed geometrical conditions due to works, incident, etc.

8. CONCLUSIONS

A macroscopic traffic flow model (META) has been successfully applied to the traffic flow of the southern part of BP which has a length of 6 km and includes five on-ramps and six off-ramps. META consists of three equations (for traffic density, mean speed, traffic volume) to be applied to each of several street sections each having a length of some 500 m. This leads to a total of 36 equations for the considered stretch of BP. Some simplifications ($\zeta = 1$, $\alpha = 1$) and some extensions (additional term for lane drop) of the model have proved to be reasonable as compared to Papageorgiou *et al.* (1989).

The modelling equations being fed with measured boundary values, traffic state inside the considered BP-stretch of 6 km is reproduced with high accuracy. The average values of error standard deviations read 10.8 km/h for mean speeds and 714 veh/h for traffic volumes. The model reproduces in a natural way complicated real traffic phenomena such as discontinuities, hysteresis phenomena, and different shapes in the diagrams of traffic variable pairs.

Six model parameters have been adjusted to real traffic conditions. In particular, the same fundamental diagram is utilized for all freeway sections with comparable geometrical characteristics. Sensitivity investigations indicate good robustness properties of the macroscopic model. The same investigations indicate that only two parameters need to be adjusted in case of application to other freeways, namely free speed v_f and critical density ρ_{cr}. Although not investigated in this study, the model is probably applicable (but less accurate) on the basis of 1 km-long sections and $T = 30$ s or more.

Application areas of the model include design and testing of sophisticated control strategies, traffic data reconstruction, analysis, simulation, and prevision of traffic flow.

Acknowledgement—The authors would like to thank the traffic engineering staff of Ville de Paris for the data material they made available for purposes of this study.

REFERENCES

Cremer M., May A. D. (1986) An extended traffic flow model for inner urban freeways. Preprints 5th IFAC/IFIP/IFORS Intern. Conf. on Control in Transportation Systems, Vienna, Austria, pp. 383–388.

Cremer M., Papageorgiou M. (1981) Parameter identification for a traffic flow model. *Automatica*, **17**, 837–843.

Grewal M. S., Payne H. J. (1976) Identification of parameters in a freeway traffic model. *IEEE Trans. on Systems, Man, and Cybernetics SMC-6*, 176–185.

Hall F. L., Gunter M. A. (1985) Further analysis of the flow-concentration relationship. *Trans. Res. Rec.*, **1091**, 1–9.

Papageorgiou M. (1983) *Applications of Automatic Control Concepts to Traffic Flow Modelling and Control*. New York, Springer-Verlag.

Papageorgiou M. (1988) Modelling and real-time control of traffic flow on the southern part of Boulevard Périphérique in Paris. Internal Report, INRETS, DART, Arcueil, France.

Papageorgiou M., Blosseville J. M., Hadj-Salem H. (1989) Macroscopic modelling of traffic flow on the Boulevard Périphérique in Paris. *Transp. Res.*, **23B**, 29–47.

Payne H. J. (1971) Models of freeway traffic and control. *Simulation Council Proc.* **1**, 51–61.

Treiterer J., Meyers J. A. (1974) The hysteresis phenomenon in traffic flow. Proc. 6th Intern. Symp. on Transportation and Traffic Theory, Sydney, Australia 13–38.